

7-2013

Finite-Temperature Micromagnetism

Ralph Skomski

University of Nebraska-Lincoln, rskomski2@unl.edu

Pankaj Kumar

Kendriya Vidhyalaya, panksamrat@gmail.com

George C. Hadjipanayis

University of Delaware, hadji@udel.edu

David J. Sellmyer

University of Nebraska-Lincoln, dsellmyer@unl.edu

Follow this and additional works at: <http://digitalcommons.unl.edu/physicskomski>

Skomski, Ralph; Kumar, Pankaj; Hadjipanayis, George C.; and Sellmyer, David J., "Finite-Temperature Micromagnetism" (2013).
Ralph Skomski Publications. 74.

<http://digitalcommons.unl.edu/physicskomski/74>

This Article is brought to you for free and open access by the Research Papers in Physics and Astronomy at DigitalCommons@University of Nebraska - Lincoln. It has been accepted for inclusion in Ralph Skomski Publications by an authorized administrator of DigitalCommons@University of Nebraska - Lincoln.

Finite-Temperature Micromagnetism

Ralph Skomski¹, Pankaj Kumar², George C. Hadjipanayis³, and D. J. Sellmyer¹

¹Department of Physics and Astronomy and NCMN, University of Nebraska, Lincoln, NE 68588 USA

²School of Basic Science, IIT Mandi, Mandi, Himachal Pradesh, India

³Department of Physics, University of Delaware, Newark, DE 19701 USA

It is investigated how magnetic hysteresis is affected by finite-temperature excitations, using soft regions in hard-magnetic matrices as model systems. In lowest order, magnetization processes are described by the traditional approach of using finite-temperature materials constants such as $K_1(T)$. Nanoscale excitations are usually small perturbations. For example, a Bloch summation over all magnon wave vectors shows that remanence is slightly *enhanced*, because long-wavelength excitations are suppressed. However, a reverse magnetic field enhances the effect of thermal excitations and causes a small reduction of the coercivity. To describe such effects, we advocate micromagnetic calculations where finite-temperature fluctuations are treated as small corrections to the traditional approach, as contrasted to full-scale Monte Carlo simulations.

Index Terms—Coercivity, finite-temperature magnetism, micromagnetism, remanence.

I. INTRODUCTION

THE temperature dependence of extrinsic magnetic properties is an important aspect of permanent magnetism, because permanent magnets are often used at and above room temperature [1]–[7]. For example, the question arises whether the soft phase in an aligned hard-soft nanocomposite may switch thermally, thereby deteriorating the permanent-magnet performance of the composite.

In lowest order, such finite-temperature fluctuations are included by using bulk values of $K_1(T)$, $M_s(T)$, and $A(T)$ in the micromagnetic energy functional [5], [8]. In the following, we will refer to this use of renormalized intrinsic materials constants as *traditional* finite-temperature micromagnetics. The use of renormalized intrinsic parameters is meaningful, because nanoscale feature sizes are generally much larger than interatomic distances [5], [9], [10]. This ensures a separation of atomic and larger “coarse-grained” length scales, and nanoscale excitations are expected to yield small corrections to the traditional micromagnetic approach.

Equilibrium nanoscale corrections, as contrasted to dynamic contributions such as sweep-rate and magnetic-viscosity corrections [3]–[5], can be tackled from different points of view. First, spin waves are generally nonnegligible for small feature sizes, for example in nanowires [11]. This is a very natural approach, because the zero-temperature nucleation mode is the lowest-lying spin-wave mode [12]. In reality, it is necessary to account for the nonuniformity of the modes [11], [13]. Second, one can approach the problem from the viewpoint of “giant fluctuations” [9], [10]. Thermal excitations are characterized by exponential terms $\exp(-E/k_B T)$, meaning that even moderate nanoscale energies yield forbiddingly small Boltzmann or Arrhenius factors. For example, the switching of an Fe region of volume $10 \times 10 \times 10 \text{ nm}^3$ in a magnetic field of 0.1 T [1 kOe] corresponds to a Zeeman-energy change of $E/k_B = 24\,800 \text{ K}$ and yields a room-temperature Boltzmann factor of 10^{-36} .

The identification of micromagnetic finite-temperature ($T > 0$) effects is not easy. This is seen by comparing model calculations [14] with finite temperature calculations such as Monte Carlo (MC) simulations [15], [16]. Almost inevitably, MC simulations yield results different from the model calculations, especially when applied to systems not adequately described by the used Hamiltonian. To identify micromagnetic finite-temperature effects, it is necessary to meet three conditions: 1) to ensure that the MC simulations agree with zero-temperature micromagnetic simulations, that is, avoiding errors due to model incompatibility, 2) to reproduce the correct $K_1(T)$, $M_s(T)$, and $A(T)$ behaviors, and 3) to subtract the results of traditional finite-temperature calculations [8] from the MC predictions. For example, it has been found [15] that magnetic dipole fields reduce the zero- and finite-temperature coercivity and remanence of hard-in-soft nanocomposites, but this is easily understood in terms of traditional numerical micromagnetics. Magnetization reductions due to dipolar effects in hard-soft-multilayers, including magnetic charges at surfaces and vortex-like curling modes [16], are also expected from micromagnetics.

In this paper, we trace nanoscale thermal contributions by comparison with exact atomistic and micromagnetic results.

II. TEMPERATURE DEPENDENCE OF ANISOTROPY

The coercivity and energy product of most permanent magnets exhibit a strong decrease with increasing temperature. For example, the relatively strong temperature dependence of the Nd^{3+} anisotropy in $\text{Nd}_2\text{Fe}_{14}\text{B}$ is a major shortcoming of this otherwise excellent material [1], [3].

Simple ferromagnets, such as Fe and Co, obey the Callen-and-Callen law [17], [18]

$$K(T) = K(0)(M_s(T)/M_s(0))^m \quad (1)$$

where $m = n(n+1)/2$ and n is the order of the anisotropy constant. For example, 2nd- and 4th-order anisotropy constants, such as uniaxial and cubic anisotropy constants K_1 , have $m = 3$ and $m = 10$, respectively.

However, the Callen and Callen model fails to describe complex magnetic materials [19], [21], and most permanent magnets strongly deviate from (1). In the rare-earth single-ion model, $K_1(T)$ is largely determined by intersublattice exchange [1],

Manuscript received November 09, 2012; revised January 24, 2013; accepted February 04, 2013. Date of current version July 15, 2013. Corresponding author: R. Skomski (e-mail: rskomski@neb.rr.com).

Color versions of one or more of the figures in this paper are available online at <http://ieeexplore.ieee.org>.

Digital Object Identifier 10.1109/TMAG.2013.2247386

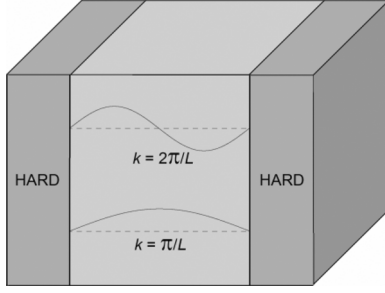


Fig. 1. Long-wavelength magnons in a nanoscale soft region (bright) embedded in a hard phase (dark).

[3], [10], whereas for $L1_0$ and actinide magnets the respective exponents m are close to 2 and 1 [21]. Due to different sublattice contributions with different temperature dependences, some ferromagnetic compounds exhibit very complicated temperature dependences of the anisotropy [3], [22], as exemplified by NdCo_5 , where K_1 has a finite-temperature zero due to competing easy-axis and easy-plane contributions [3].

Another example is sintered Sm-Co, where the 2:17 main phase is surrounded by a Cu-rich 1:5 grain-boundary phase [23], and additives such as Cu and Ti can be used to tune the coercivity. Some of these materials exhibit a maximum $H_c(T)$ at some temperature [7], [24]. The maximum reflects a change in pinning strength due the different temperature dependences of the involved phases [24] and eventual grain isolation, as opposed to giant micromagnetic fluctuations. For example, putting $T = 0$ in the hypothetical expression $H_c \sim \exp(\Delta E/k_B T)$ corresponds to unphysically high energy barriers ΔE and yields an unphysical divergence of H_c at $T = 0$ [9], [10].

III. EFFECTS OF SPIN WAVES

The spin-wave corrections are obtained by performing Bloch summations and subsequently comparing the results with bulk properties. We have performed explicit model calculations for soft regions in a hard matrix, a case typical of hard-soft nanostructures, and show that the remanence of the soft phase is actually slightly higher than in the bulk. This is because the boundary conditions at the hard-soft boundary suppress long-wavelength spin waves.

Fig. 1 explains nanoscale spin-wave excitations in a nanostructure, namely in a soft region of dimension L (white) embedded in a hard matrix (gray). Compared to infinite soft magnets, long-wavelength magnons ($k > \pi/L$) are suppressed.

Let us describe the soft phase (Fe) by the Heisenberg Hamiltonian

$$\mathbf{H} = -\frac{1}{S^2} \sum_{i>j} J_{ij} \mathbf{S}_i \cdot \mathbf{S}_j - 2\mu_o \mu_B \sum_i \mathbf{H} \cdot \mathbf{S}_i. \quad (2)$$

Its mean-field treatment amounts to the neglect of fluctuations, $C_{ij} = (\mathbf{S}_i - \langle \mathbf{S}_i \rangle) \cdot (\mathbf{S}_j - \langle \mathbf{S}_j \rangle)$. With $\mathbf{S}_i \cdot \mathbf{S}_j = \mathbf{S}_i \cdot \langle \mathbf{S}_j \rangle + \langle \mathbf{S}_i \rangle \cdot \mathbf{S}_j + C_{ij}$ it is easy to show that the mean-field theory amounts to the replacement $J\mathbf{S}_i \cdot \mathbf{S}_j \rightarrow 2J\mathbf{S}_i \cdot \langle \mathbf{S}_j \rangle$. The corresponding mean-field Curie temperature is obtained from $\langle S_z \rangle =$

$S B_S(2\mu_o \mu_B H_{MF} S/k_B T)$, and $H_{MF} = zJ\langle S_z \rangle/2\mu_o \mu_B S^2$. Explicitly, $T_c = (S + 1)zJ/3Sk_B$, $A = zJ\Delta R^2/12V_{at}$, where $\Delta R = 2R_{at}$ is the interatomic distance.

The low-temperature behavior of isotropic Heisenberg magnets, (2), is determined by spin-waves (magnons). In hard magnets, an anisotropy must be added to this equation, but our focus is on the soft phase. At low temperatures, the magnons are non-interacting, and the total energy $E = \sum_{\mathbf{k}} n_{\mathbf{k}} E_{\mathbf{k}}$ with the well-known dispersion relation

$$E_{\mathbf{k}} = 2\mu_o \mu_B H_z + \frac{J}{S} a^2 k^2. \quad (3)$$

This equation, where a is the lattice parameter, is valid for sc, bcc, and fcc lattices, but not for more complicated crystal structures. A more general expression is $E_{\mathbf{k}} = 2\mu_o \mu_B H + zJk^2 \Delta R^2/6S$. Note that sc, bcc, and fcc lattices have volumes V_{at} per atom of a^3 , $a^3/2$, and $a^3/4$, respectively, whereas the interatomic distances $\Delta R = 2R_{at}$ obey the respective relations $\Delta R^2 = a^2$, $\Delta R^2 = 3a^2/4$, and $\Delta R^2 = a^2/2$. As a consequence, the quantity $z\Delta R^2 = 6a^2$ is the same for all three lattices.

The average magnetization, $M(T)/M_o = \langle S_z \rangle/S$ is given by

$$\frac{M(T)}{M_o} = 1 - \frac{1}{N} \sum_{\mathbf{k}} n_{\mathbf{k}} \quad (4)$$

where N is the number of atomic spins. With

$$n_{\mathbf{k}} = 1/(\exp(E_{\mathbf{k}}/k_B T) - 1) \quad (5)$$

and $\sum_{\mathbf{k}} \dots = (V/8\pi^3) \int \dots d\mathbf{k}$, where $V = NV_o$ is the total volume, this becomes

$$\frac{M(T)}{M_o} = 1 - \frac{V_o}{8\pi^3 S} \int \frac{1}{\exp(E_{\mathbf{k}}/k_B T) - 1} d\mathbf{k}. \quad (6)$$

Here $M_o = M_s(0)$ is the zero-temperature spontaneous magnetization. It is convenient to make the expressions in the integral dimensionless, by introducing $\eta = (Ja^2/Sk_B T)^{1/2} k$ and $b = 2\mu_o \mu_B H_z$. This yields

$$\frac{M(T)}{M_o} = 1 - \frac{\sqrt{S}}{2\pi^2 n_o} \left(\frac{k_B T}{J} \right)^{3/2} \int_{\eta_{\min}}^{\eta_{\max}} \frac{\eta^2}{\exp(\eta^2 + b) - 1} d\eta. \quad (7)$$

For $b = 0$ ($H = 0$), $\eta_{\min} = 0$, and $\eta_{\max} = \infty$, we can exploit that

$$\int_0^{\infty} \frac{x^2}{\exp(x^2) - 1} dx = \frac{\sqrt{\pi}}{4} \zeta(3/2) \quad (8)$$

and $\zeta(3/2) = 2.612$. This reproduces Bloch's law

$$\frac{M(T)}{M_o} = 1 - \frac{c\sqrt{S}}{n_o} \left(\frac{k_B T}{J} \right)^{3/2} \quad (9)$$

where $c = \zeta(3/2)\sqrt{\pi}/8\pi^2 = 0.0586$.

The long-wavelength cutoff η_{\min} describes the nanoscale effects of interest in this paper. In the absence of a magnetic field

($b = 0$), the term $\exp(\eta^2)$ can be replaced by $1 + \eta^2$, because the long-wavelength nanoscale modes of interest in the present context are not frozen. Very low temperatures, such as 4.2 K, would require a more subtle treatment, but such low temperatures go beyond the purpose of this paper, as do temperatures near the Curie point.

Since modes with $k < \pi/L$ do not contribute to the thermal magnetization reduction, the integral in (7) extends from $\eta_{\min} \sim 1/L$ to $\eta_{\max} \sim 1/a$, as contrasted to $\eta_{\min} = 0$ for bulk modes. The difference is of the order of a/L . Taking $a = 0.25$ nm and $L = 10$ nm yields a correction of 2.5% to $M_o - M_s(T)$. Since $M_o - M_s(T) \ll M_o$, the relative correction to $M_s(T)$ is much smaller, hardly more than a few 0.1%. In other words, harmful long-wavelength excitations are not excited due to geometrical constraints, and the nanostructuring *enhances* the spontaneous magnetization.

IV. BEHAVIOR NEAR COERCIVITY

As in other areas of physics, thermal fluctuations are most important near phase transitions and other instabilities. A well-known example is the critical point at the Curie temperature T_c , where the correlation length becomes comparable to the nanoscale feature sizes. This effect is limited to the immediate vicinity of T_c [5], but a similar mechanism exists for the destabilization of the magnetization direction due to a reverse magnetic field (nucleation). The corresponding equilibrium fluctuations around local free energy minima add to the above-mentioned sweep-rate dependence of the coercivity. This tends to reduce the coercivity, but the corresponding change in coercivity is very small, less than about 1%.

Let us consider the low-temperature limit of small magnetization fluctuations $\mathbf{M} - M_o \mathbf{e}_z = m_x \mathbf{e}_x + m_y \mathbf{e}_y$. For uniaxial symmetry, the x and y directions are equivalent, and the energy of the fluctuations in a reverse field $\mathbf{H} = -H \mathbf{e}_z$ can be written as [3], [5], [25]

$$E = \int [A(\nabla m)^2 + (K_1(r) - \mu_o M_s H/2)m^2] dV. \quad (10)$$

Here $A = zJ\Delta R^2/12V_{\text{at}}$ is the spin-wave stiffness, typically of the order of 10^{-11} J/m. Consider a cubic soft region of volume L^3 in a very hard matrix. At zero temperature, the nucleation eigenmode

$$m = m_o \cos(x\pi/L) \cos(y\pi/L) \cos(z\pi/L) \quad (11)$$

corresponds to a nucleation field $H_o = 6\pi^2 A/\mu_o M_o^2 L^2$. Note that (11) is valid for large L and describes the hard-soft exchange in terms of clamped [26] boundary conditions. Small L require more complicated boundary conditions [14] and yield a more bulk-like behavior. In traditional micromagnetics, A and M_o are replaced by their finite-temperature values, but this does not account for nanoscale excitations.

Putting (11) into (10) yields

$$E = m_o^2 (3\pi^2 AL/8 - \mu_o M_o HL^3/16). \quad (12)$$

The thermally averaged magnitude of the fluctuations is obtained from the probability $p(m_o) = Z^{-1} \exp(-E(m_o)/k_B T)$.

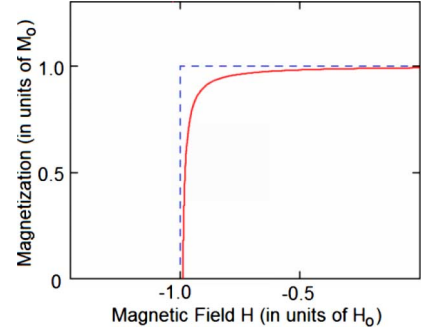


Fig. 2. Thermal effect on coercivity of an embedded soft region, as described by (13). Both curves are for the soft-phase magnetization—the total $M(H)$ curve looks more rectangular.

The integration $\langle m_o^2 \rangle = \int m_o^2 p(m_o) dm_o$ is straightforward and yields

$$\langle m_o^2 \rangle = \frac{k_B T}{3\pi^2 AL/4 - \mu_o M_s HL^3/8}. \quad (13)$$

This means that $\langle m_o^2 \rangle \sim M_z$ scales as $1/(H_o - H)$. Small values of $\langle m_o^2 \rangle$ are inconsequential, because m fluctuates forth and back. Magnetization reversal occurs close to the field where the magnetization in the center of the cube is in the x - y -plane, that is, when $\langle m_o^2 \rangle = 1$. This yields

$$H_c = H_o \left(1 - \frac{8k_B T}{6\pi^2 AL} \right) \quad (14)$$

that is, a very small correction to H_o , as shown in Fig. 2. For example, taking $T = 300$ K, $A = 10$ pJ/m, and $L = 10$ nm, we obtain a coercivity reduction by 0.56%.

V. DISCUSSION

Finite-temperature micromagnetic calculations can, in principle, be performed by MC simulations [16], [27], but these calculations require a reasonable starting Hamiltonian. Simple ferromagnets, such as elemental Fe and Co, are easy to model, but hard-magnetic rare-earth transition-metal (RE-TM) intermetallics have drastically different temperature dependences. Fig. 3 illustrates this point for NdCo_5 , where the strongly negative Nd sublattice contribution yields easy-plane anisotropy at low temperatures. However, due to Nd^{3+} intramultiplet excitations, the rare-earth anisotropy rapidly decreases with temperature, and at room temperature and above, the smaller but positive and less temperature-dependent Co sublattice anisotropy dominates. This yields spin-reorientation transition (anisotropy zero) at $T_{\text{SRT}} \approx 280$ K [3], where the material is magnetically very soft.

The effect can be rationalized by considering the hysteresis of a soft-in-hard nanoparticle, Fig. 3(a). We have employed the Nmag software package [28] to perform micromagnetic hysteresis-loop calculations for $A = 10$ pJ/m, $\mu_o M(\text{NdCo}_5) = 1.23$ T, $K_1(T_{\text{SRT}}) = 0$ and $K_1(T_{\text{SRT}} + 25 \text{ K}) = 0.7$ MJ/m, using Fe as the soft phase ($\mu_o M_s = 2.15$ T). Fig. 3(b) shows two hysteresis loops. The qualitative difference between the two loops, namely as a change from a hard-soft composite to a soft-magnetic particle at T_{SRT} , is easy to understand from a

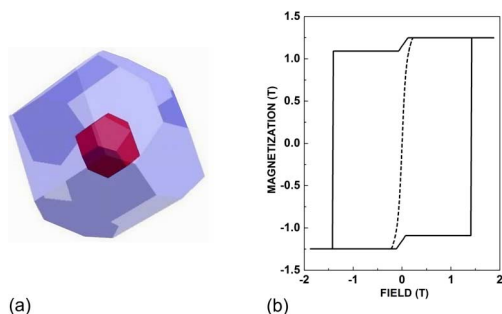


Fig. 3. Temperature dependence of the hysteresis of a soft-in-hard composite NdCo_5 : Fe nanoparticle of size 14.8 nm with an Fe core of diameter 5 nm: (a) structure and (b) hysteresis loops at T_{SRT} (dashed line) and 25 K above T_{SRT} (solid line).

micromagnetic point of view but not reproduced by present-day MC simulations.

This shows that traditional finite-temperature micromagnetic calculations are superior in the sense that they automatically include complicated intrinsic phenomena. Adding realistic $K_1(T)$ dependences to nanoscale MC calculations is a substantial challenge, and any attempt to perform such a calculation would probably mean that most of the computational time is used to reproduce the atomic-scale quantum mechanics of anisotropy (intramultiplet excitations), rather than taking the result $K_1(T)$ of these excitations as an input. In fact, this challenge has been one of the motivations behind multiscale modeling [27]. Similarly, in [16], the spin-wave stiffness is convoluted with long-range dipolar forces, which indicates problems on a basic micromagnetic level.

VI. CONCLUSION

In summary, we have investigated how nanoscale thermal excitations affect the hysteresis of hard-soft nanocomposites. Due to a long-wavelength cutoff, the remanence slightly increases compared to traditional micromagnetic calculations, but thermal effects become more important in reverse fields, and the coercivity is somewhat reduced. To adequately describe nanoscale thermal effects, we advocate to start from “renormalized” traditional micromagnetic calculations, complemented by magnon-like normal-mode perturbations. Compared to MC simulations based on simplified magnetic models, this ensures that all lowest-order effects are properly taken into account.

ACKNOWLEDGMENT

This research was supported by the Delaware ARPA-E (DJS, GCH), NSF MRSEC (DMR-0820521, RS), DST (PKS), and NCMN. The authors would like to thank P. Manchanda and A. Kashyap for discussing computational details.

REFERENCES

[1] J. F. Herbst, “ $\text{R}_2\text{Fe}_{14}\text{B}$ materials: Intrinsic properties and technological aspects,” *Rev. Mod. Phys.*, vol. 63, pp. 819–898, 1991.

[2] *Concise Encyclopedia of Magnetic and Superconducting Materials*, J. E. Evetts, Ed. Oxford, U.K.: Pergamon, 1992.

[3] R. Skomski and J. M. D. Coey, *Permanent Magnetism*. Bristol, U.K.: Inst. Phys., 1999.

[4] T. Leineweber and H. Kronmüller, “Dynamics of magnetisation states,” *J. Magn. Magn. Mater.*, vol. 192, pp. 575–590, 1999.

[5] R. Skomski, “Nanomagnetics,” *J. Phys.: Condens. Matter*, vol. 15, pp. R841–896, 2003.

[6] C. H. Chen, M. S. Walmer, M. H. Walmer, S. Liu, E. Kuhl, and G. Simonet, “ $\text{Sm}_2(\text{Co,Fe,Cu,Zr})_{17}$ magnets for use at temperature $\geq 400^\circ\text{C}$,” *J. Appl. Phys.*, vol. 83, pp. 6706–6708, 1998.

[7] S. Liu, J. Yang, G. Doyle, G. Potts, and G. E. Kuhl, “Abnormal temperature dependence of intrinsic coercivity in sintered Sm-Co-based permanent magnets,” *J. Appl. Phys.*, vol. 87, pp. 6728–6730, 2000.

[8] T. Schrefl and J. Fidler, “Micromagnetic simulation of magnetizability of nanocomposite Nd-Fe-B magnets,” *J. Appl. Phys.*, vol. 83, p. 6262, 1998.

[9] R. Skomski, “Role of thermodynamic fluctuations in magnetic recording (invited),” *J. Appl. Phys.*, vol. 101, pp. 09B104-1–09B104-6, 2007.

[10] R. Skomski, *Simple Models of Magnetism*. Oxford, U.K.: Oxford Univ. Press, 2008.

[11] R. Skomski, M. Chipara, and D. J. Sellmyer, “Spin-wave modes in magnetic nanowires,” *J. Appl. Phys.*, vol. 93, pp. 7604–7606, 2003.

[12] A. Aharoni, *Introduction to the Theory of Ferromagnetism*. Oxford, U.K.: Oxford Univ. Press, 1996.

[13] F. Vidal, Y. Zheng, P. Schio, F. J. Bonilla, M. Barturen, J. Milano, D. Demaille, E. Fonda, A. J. A. de Oliveira, and V. H. Etgens, “Mechanism of localization of the magnetization reversal in 3 nm wide Co nanowires,” *Phys. Rev. Lett.*, vol. 109, pp. 117205-1–117205-2, 2012.

[14] R. Skomski and J. M. D. Coey, “Giant energy product in nanostructured two-phase magnets,” *Phys. Rev.*, vol. B 48, pp. 15812–15816, 1993.

[15] A. M. Belemuk and S. T. Chui, “Comparative study of finite temperature demagnetization in $\text{Nd}_2\text{Fe}_{14}\text{B}$ and SmCo_5 based hard-soft composites,” *J. Appl. Phys.*, vol. 110, pp. 073918-1–073918-7, 2011.

[16] A. M. Belemuk and S. T. Chui, “Temperature-dependent demagnetization behaviour in perpendicular exchange-coupled $\text{SmCo}_5/\text{FeCo}$ multilayers,” *J. Phys. D: Appl. Phys.*, vol. 45, pp. 125001-1–125001-14, 2012.

[17] N. Akulov, “Zur Quantentheorie der Temperaturabhängigkeit der Magnetisierungskurve,” *Z. Phys.*, vol. 100, pp. 197–202, 1936.

[18] E. R. Callen, “Temperature dependence of ferromagnetic uniaxial anisotropy constants,” *J. Appl. Phys.*, vol. 33, pp. 832–835, 1962.

[19] R. Skomski, “Exchange-controlled magnetic anisotropy,” *J. Appl. Phys.*, vol. 91, pp. 8489–8491, 2002.

[20] R. Skomski, A. Kashyap, and D. J. Sellmyer, “Finite-temperature anisotropy of PtCo magnets,” *IEEE Trans. Magn.*, vol. 39, no. 5, pp. 2917–2919, 2003.

[21] R. Skomski, O. N. Mryasov, J. Zhou, and D. J. Sellmyer, “Finite-temperature anisotropy of magnetic alloys,” *J. Appl. Phys.*, vol. 99, pp. 08E916-1–08E916-4, 2006.

[22] *Rare-Earth Iron Permanent Magnets*, J. M. D. Coey, Ed. Oxford, U.K.: Oxford Univ. Press, 1996.

[23] K. Kumar, “ RETM_5 and $\text{RE}_2\text{TM}_{17}$ permanent magnets development,” *J. Appl. Phys.*, vol. 63, pp. R13–57, 1988.

[24] J. Zhou, R. Skomski, C. Chen, G. C. Hadjipanayis, and D. J. Sellmyer, “Sm-Co-Ti high-temperature permanent magnets,” *Appl. Phys. Lett.*, vol. 77, pp. 1514–1516, 2000.

[25] H. Kronmüller and H. R. Hilzinger, “Incoherent nucleation of reversed domains in Co_5Sm permanent magnets,” *J. Magn. Magn. Mater.*, vol. 2, pp. 3–10, 1976.

[26] R. Skomski, J.-P. Liu, and D. J. Sellmyer, “Quasicoherent nucleation mode in two-phase nanomagnets,” *Phys. Rev. B*, vol. 60, pp. 7359–7365, 1999.

[27] O. N. Mryasov, U. Nowak, K. Y. Guslienko, and R. W. Chantrell, “Temperature-dependent magnetic properties of FePt: Effective spin Hamiltonian model,” *Europhys. Lett.*, vol. 69, pp. 805–811, 2005.

[28] T. Fischbacher, M. Franchin, G. Bordignon, and H. Fangohr, “A systematic approach to multiphysics extensions of finite-element-based micromagnetic simulations: Nmag,” *IEEE Trans. Magn.*, vol. 43, no. 6, pp. 2896–2898, 2007.